



**Numerical Modeling and Multi-Parameter study of Porous Media Packed-Bed
Latent Heat Thermal Energy Storage Systems**

Lappeenranta–Lahti University of Technology LUT

Bachelor's Programme in Energy Technology, Bachelor's thesis

2026

Tianlin Zhang

Examiner(s): Professor Hongzhi Yan

Markus Secomandi, M.Sc. (Tech.)

ABSTRACT

Lappeenranta–Lahti University of Technology LUT

LUT School of Energy Systems

Energy Technology

Hebei University of Technology

Tianlin Zhang

Numerical Modeling and Multi-Parameter study of Porous Media Packed-Bed Latent Heat Thermal Energy Storage Systems

Bachelor's thesis

2026

43 pages, 19 figures, 10 tables

Examiner(s): Professor Hongzhi Yan and Markus Secomandi, M.Sc. (Tech.)

Keywords: porous media; packed-bed latent heat storage; phase change material; local thermal non-equilibrium; numerical modeling; multi-parameter improvement

This investigation looked at using packed-bed thermal energy storage (TES) systems with phase-change materials (PCM) to improve the efficiency of latent heat storage in solar thermal systems. The effects of the diameter of the particles in the bed, the porosity of the bed, the inlet temperature and the heat flux on the time to charge the system, the propagation of the thermal front, and the change in the liquid fraction were analyzed using numerical simulations under local thermal non-equilibrium (LTNE) conditions. The results indicated that the melting was not uniform along the bed, that the fluid was responsive to heat earlier than the solid matrix, and that the process of phase change occurred differently at different locations in the bed. The results will assist in developing an optimized design for TES, improving the charge performance of TES, and increasing the energy density and power output from the packed-bed PCM system.

SYMBOLS AND ABBREVIATIONS

Roman characters

$D(p)$	particle diameter	mm, m
$F(\text{liq})$	liquid fraction	-
h	heat transfer coefficient	$\text{W}/(\text{m}^2 \cdot \text{K})$
k	thermal conductivity	$\text{W}/(\text{m} \cdot \text{K})$
P	pressure	Pa
$P(\text{atm})$	atmospheric pressure	Pa
$Q(u)$	solar heating power / heating power input	W
$Q(v)$	volumetric heat storage power	W/m^3
t	time	s, h
T	temperature	K
u	velocity	m/s

Greek characters

ΔP	pressure drop	Pa
ΔT	temperature difference	K
$\varepsilon (\text{por})$	porosity	-
μ	dynamic viscosity	$\text{Pa} \cdot \text{s}$
ρ	density	kg/m^3

Dimensionless quantities

Re	Reynolds number	-
----	-----------------	---

Subscripts

f	fluid phase
s	solid phase
pcm	phase change material
liq	liquid phase
atm	atmospheric
u	useful / input heating

Abbreviations

CFD	Computational Fluid Dynamics
COMSOL	COMSOL Multiphysics
HTF	Heat Transfer Fluid
LHTES	Latent Heat Thermal Energy Storage
LTE	Local Thermal Equilibrium
LTNE	Local Thermal Non-Equilibrium
PCM	Phase Change Material
TES	Thermal Energy Storage

Table of contents

Abstract

Declarations

1	Introduction.....	7
1.1	Research Background and Significance.....	7
1.2	Research Questions to Be Discussed	7
1.3	Objective of the Thesis.....	8
2	Literature Review and Theoretical Background	9
2.1	Overview of Thermal Energy Storage Technologies.....	9
2.2	Classification and Selection of Phase Change Materials	10
2.3	Overview of Porous Media Systems	10
2.4	Influence of Structural Parameters.....	11
2.4.1	Influence of Capsule Size and Particle Diameter	11
2.4.2	Bed Porosity and Packing Structure	12
2.5	Phase Change Heat Transfer Mechanism and Liquid Fraction.....	13
2.6	Influence of Solar Heating Power	14
3	Methodology and Evaluation Framework	15
3.1	Structural Description of the Packed Bed Latent Heat Storage System	15
3.2	Basic Modeling Assumptions.....	16
3.3	Numerical Solution Method and Software Platform.....	16
3.4	Geometric Model and Mesh Division	17
3.5	Initial Conditions and Model Setup	18
4	Results and Discussion	19
4.1	Baseline Data Results.....	19
4.1.1	Volumetric Heat Storage Density.....	21
4.1.2	Volumetric Heat Storage Power	22
4.2	Improvement-Oriented Analysis	23
4.2.1	Theoretical Hypothesis	23
4.2.2	Actual Data Analysis	24
4.2.3	Improvement of Volumetric Heat Storage Density.....	25
4.2.4	Expansion of the Sensible Heat Temperature Difference	27
4.2.5	Updated Volumetric Heat Storage Density Results	28
4.2.6	Improvement of Volumetric Heat Storage Power	30
4.2.7	Improved Data	31
4.3	Influence of Particle Diameter and Porosity	32
5	Pressure loss assessment	35
5.1	Definition of Pressure Drop and Validation Criterion	35
5.2	Pressure Drop Calculation Model (Ergun Equation)	36
5.3	Parameter Substitution and Calculation Process.....	36
5.4	Pressure Drop Results and Table Summary	37
5.5	Discussion of Limitations and Uncertainties	38
6	Conclusion	39
7	References.....	41

DECLARATIONS

Turnitin

The originality of this thesis has been reviewed with the Turnitin similarity checking service.

AI usage

The author of the thesis, Tianlin Zhang, used the following AI-tools during the preparation of the thesis:

1. Chatgtp
 - a. Purpose of use: To translate some special proper nouns and translate the background of the literature review and long paragraphs from Chinese into English.
 - b. Explanation of the use of the tool: Because the base version of my thesis was written in Chinese, I used a translation tool to translate it.
2. Youdao
 - a. Purpose of use: To translate some special proper nouns and translate the background of the literature review and long paragraphs from Chinese into English.
 - b. Explanation of the use of the tool: Because the base version of my thesis was written in Chinese, I used a translation tool to translate it.

Responsibility

The author, Tianlin Zhang, takes full responsibility for the content of this thesis and has reviewed and edited the content generated by the possible use of AI tools.

1 Introduction

Thermal energy storage (TES) with the use of phase change materials (PCM) is receiving a lot of research and attention in the area of improving how we use renewable energy sources. However, there are still some challenges associated with their characteristics (e.g., non-uniform melting) and limitations to heat transfer that require more study.

1.1 Research Background and Significance

With the increasing share of renewable energy, thermal systems increasingly face supply fluctuations and rigid heat demand. TES is therefore an important means of improving flexibility and shifting heat across time scales (Hilmi et al., 2023; Wu et al., 2024; Wu et al., 2026).

In district heating systems, supply and return temperature constraints often cause supply-demand mismatch, heat curtailment, and unstable operation. Locating storage units at substations has therefore become an important strategy for peak shaving and temperature stabilization (Hilmi et al., 2023; Wu et al., 2024; Wu et al., 2026).

Compared with sensible heat storage in large water tanks, PCM-based latent heat storage provides higher energy density within a smaller temperature interval and is more suitable for compact applications requiring stable output temperatures. Engineering studies have shown that PCM storage units can mitigate supply-demand mismatch and improve thermal-system efficiency (Bentivoglio et al., 2023; Wu et al., 2024; Wu et al., 2026).

1.2 Research Questions to Be Discussed

Packed bed latent heat storage systems are affected by a multiplicity of interactions between their various factors; thus, this study explores the main factors of packed bed latent heat storage systems. Factors such as bed porosity, particle diameter, fluid flow rate/velocity, solar heating power and heat transfer fluid mass have been evaluated and subjected to systematic analysis to determine how each of these factors affect the storage process. The questions for this study will include the following:

- A. How changes in each parameter affect phase change propagation rate, bed temperature uniformity, and the time to complete phase change and store heat.
- B. The sensitivity ranking of each parameter.
- C. Whether there are synergistic (“co-enhancing”) or counteracting (“mutually cancelling”) interactions among parameters.

1.3 Objective of the Thesis

Building off of the existing trade-offs of influences of influencing, this paper investigates how to find feasible optimal parameter combinations for engineering. In addition to being optimized from a performance perspective, engineering constraints must also be satisfied within that process (e.g., maximum power levels of the heat source, acceptable manufacturing capabilities of the structure(s), acceptable operational stability of the engineering systems, and maximum safe temperatures).

In this regard, the research specifically outlines improvement purpose (i.e., to reduce the amount of time spent to complete the phase change, increase the energy contained in the stored energy versus its density, increase the amount of time that can be stored at a particular rate of storage, and the phrase is used to cover several different types of application objectives), organizes a common basis for comparison and evaluation, and develops a multi-parameters coordinated method with respect to each other under constraint type conditions. Finally, the research develops practical design and operation suggestions from the results of this investigation, including possible matches between particle diameter/porosity/flow/principal power, the suggested range and combinations of properties, and possible selection methods for each application’s overall objectives.

2 Literature Review and Theoretical Background

Packed-bed phase change material (PCM) thermal energy storage (TES) systems provide a high density of stored energy based on their thermal, and they also have a lot of potential to be a part of renewable energy systems. Therefore, understanding the charging process and the limitations to heat transfer for PCM systems is very important to ensure that PCM TES systems work well and perform well for their intended applications.

2.1 Overview of Thermal Energy Storage Technologies

From the viewpoint of energy storage methodologies, TES types can be generally categorized into three categories: Sensible heat (e.g., using temperature variation to store) Latent heat (e.g., through use of phase change latent heat) Thermochemical (e.g., through reversal of reactions).

In terms of specific device configurations, packed beds are widely used in both sensible and latent heat storage due to their simple structure, controllable cost, modularity, and scalability. The basic concept of a packed bed is to fill the bed layer with solid particles (such as rocks, ceramics, metals, or encapsulated PCM capsules) and allow a heat transfer fluid (HTF) to flow through the bed pores and exchange heat with the particles, thereby promoting the propagation of the internal temperature wave (thermocline). The performance of the packed bed largely depends on the synergistic interaction between bed structure and flow–heat transfer processes (Georgousis et al., 2025; He et al., 2022).

For latent heat packed beds, Figure 1 shows the PCM encapsulation form (spherical capsules, cylindrical capsules, honeycomb modules, etc.) determines the evolution of the phase interface, the degree of natural convection, and the effective thermal conduction path. Meanwhile, bed porosity, particle size, distributor design, and boundary operation conditions govern flow distribution, pressure drop, and the maintenance of heat transfer driving force.

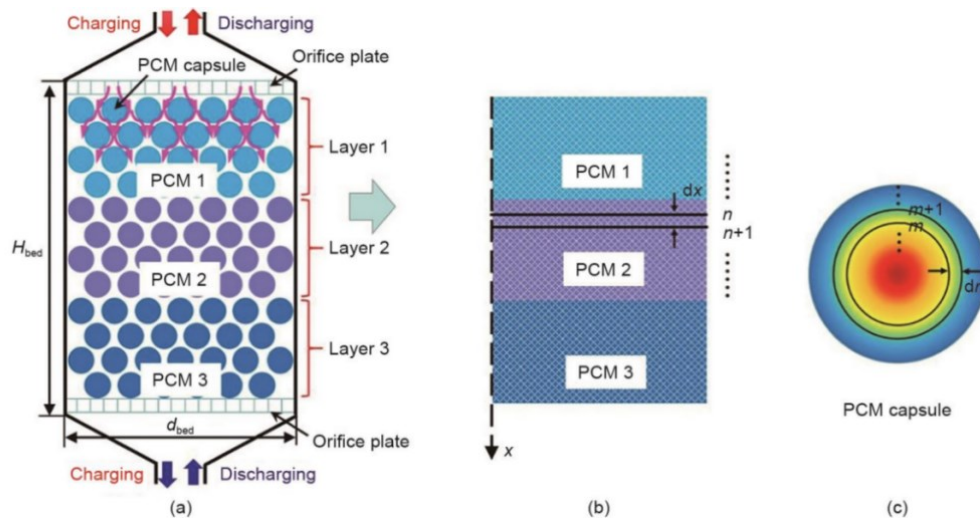


Figure 1. Latent heat packed beds(Zhang et al., 2023)

2.2 Classification and Selection of Phase Change Materials

PCMs are generally classified according to material type into organic (such as paraffins, fatty acids), inorganic (such as hydrated salts, metals/eutectic systems), and eutectic materials. When selecting a PCM, comprehensive considerations are generally required, including phase change temperature matching, latent heat, specific heat, thermal conductivity, volume change, supercooling tendency, cyclic stability, compatibility/corrosion, safety, and cost (He et al., 2022; Karthikeyan et al., 2024).

In medium- and low-temperature heating and domestic hot water temperature ranges, paraffin-based organic PCMs are widely used due to their chemical stability, tunable phase change temperature through carbon chain modification, relatively low supercooling, low corrosivity, and wide availability.

2.3 Overview of Porous Media Systems

Latent Heat Thermal Energy Storage (LHTES) utilizes materials to absorb or release large amounts of latent heat during phase change, achieving high-density energy storage. As a typical application form of PCM, porous media packed beds offer advantages of simple structure, modular scalability, and controllable cost (He et al., 2022; Karthikeyan et al., 2024).

Packed bed systems are generally composed of PCM capsules and a HTF. Figure 2 shows the bed pores and exchanges heat with the PCM capsules, enabling charging

and discharging of the bed (He et al., 2022; Karthikeyan et al., 2024). Compared with sensible heat storage, latent heat storage can store large amounts of energy over a small temperature difference in the phase change region, making the system compact and stable. Researchers have focused on the influence of PCM thermal properties, phase change temperature, encapsulation method, and bed structure on heat transfer efficiency.

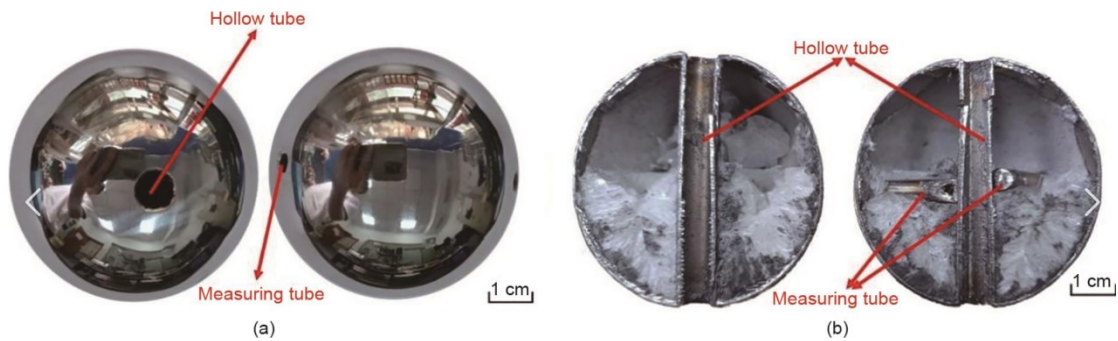


Figure 2. Near-spherical capsule (Zhang et al., 2023)

In recent years, research on packed bed LHTES systems has gradually expanded from single-layer performance to system-level applications, including solar hot water, industrial waste heat recovery, and district heating system (Avargani et al., 2021; David-Hernández et al., 2024; Wu et al., 2024; Wu et al., 2026; Yao et al., 2026).

2.4 Influence of Structural Parameters

The structural parameters of packed beds for latent heat storage mainly include capsule geometric dimensions (diameter, shell thickness, shape), bed porosity and packing method, bed aspect ratio, and distributor/manifold structure. These parameters influence the specific surface area, effective thermal conduction paths, local velocity distribution, and temperature wavefront within the bed, ultimately affecting the charging/discharging time, temperature platform stability, and pressure drop of the device (He et al., 2022; Karthikeyan et al., 2024).

2.4.1 Influence of Capsule Size and Particle Diameter

Most studies under similar boundary conditions have reached a consistent conclusion: reducing capsule diameter typically increases the unit volume heat transfer area, accelerating phase change progression and shortening the time required for the bed outlet to reach the target temperature platform. By maximising the number of capsules

with fewer pore channel connections (base on the Figure 3) then increasing pressure drop and imposing greater requirements for distributor safety on the system will occur (He et al., 2022; Karthikeyan et al., 2024).

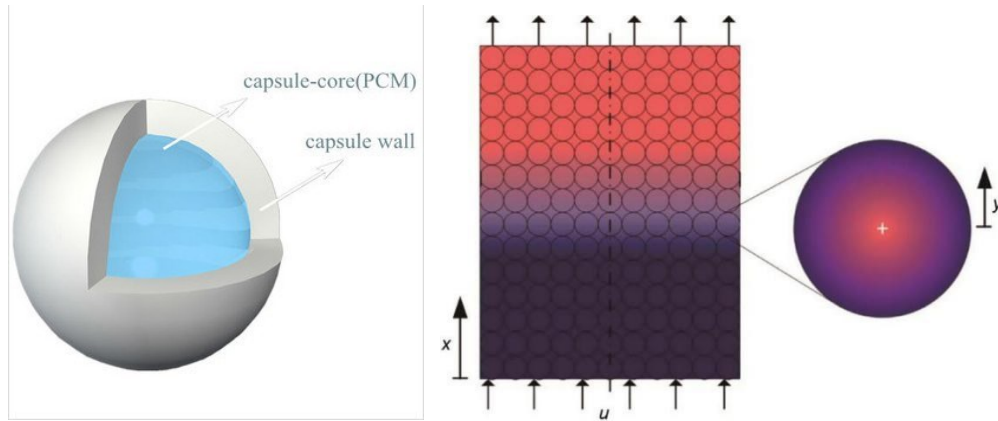


Figure 3. Arrangement structure of the capsule (Zhang et al., 2023)

Capsule size, or particle diameter, is therefore a key parameter affecting charging and discharging rates. Extremely small particles may reduce the relative contribution of fluid–solid convection, making heat conduction dominant and generating local micro-scale thermal resistance. At the same time, smaller particles significantly increase flow resistance, which places higher demands on HTF distribution and system pumping. Therefore, particle diameter should be carefully engineered to balance rapid heat transfer and flow resistance, so that charging/discharging efficiency and system energy consumption can be optimized simultaneously (Chen et al., 2024; He et al., 2022; Karthikeyan et al., 2024).

2.4.2 Bed Porosity and Packing Structure

Figure 4 shows that bed porosity not only determines the filling amount of PCM capsules, but also directly affects fluid flow, local heat transfer, and temperature field distribution. In porous media packed beds, changes in porosity influence system performance in multiple ways. First, a high porosity reduces fluid resistance, improves flow uniformity, and enhances convective heat transfer, particularly in the downstream region of the bed, which can effectively improve the uniformity of liquid fraction distribution and phase change propagation. However, excessively high porosity reduces the unit volume PCM filling, lowering the system’s thermal density and potentially affecting thermal compactness. Conversely, low porosity increases

bed resistance, forming local dead zones and potentially leaving some PCM untransformed, thereby reducing overall thermal storage efficiency (Karthikeyan et al., 2024; Wang, 2025; Wu et al., 2024).

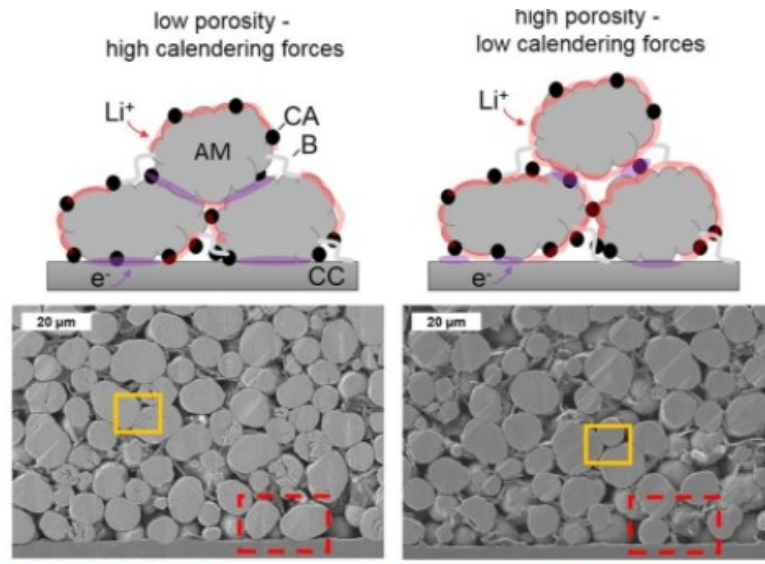


Figure 4. Bed porosity and the filling structure of PCM capsules (Zhang et al., 2023)

Regarding packing strategy, studies have shown that layered or gradient packing can form temperature gradients at different bed positions, alleviating uneven propagation of the thermal front (Chen et al., 2024; Wang, 2025; Yao et al., 2026).

2.5 Phase Change Heat Transfer Mechanism and Liquid Fraction

The charging and discharging of PCM predominantly consists of three distinct temperature modes - sensible heat increase or decrease, latent heat exchanged and sensible heat after the phase change. While the phase change in a packed bed typically displays a series of irregularities, the distribution of liquid fractions within the bed will indicate whether a phase change is occurring or not. Local thermal non-equilibrium (LTNE) theory suggests that fluid temperatures rise sooner than the solid temperatures due to a lag in the response of solids. This produces thermal platforms and slopes that illustrate the characteristics of latent heat being absorbed or released in the packed bed (Embiale et al., 2025; He et al., 2022).

The liquid fraction serves as one of the key indicators of what percentage of the phase change material (PCM) has gone through its phase change process. A high liquid

fraction also means that the latent heat has been completely discharged and, therefore provides a very effective thermal storage capacity for that system. The liquid fraction of the PCM in a thermal storage system has a spatial distribution which can vary based on bed structure, diameter of the PCM particles, porosity, rate of fluid flow and rate of heat transfer; in the literature, researchers have indicated that by optimizing a combination of capsule size and porosity, the liquid fraction distribution can be made more uniform; in addition, the number of partially untransformed areas will be reduced and the reliability of the thermal storage system will increase along with its dynamic response capabilities (He et al., 2022; Karthikeyan et al., 2024).

2.6 Influence of Solar Heating Power

Solar thermal energy has a substantial impact on the abilities of the PCM to change its phase and produce liquid when subjected to sufficient solar thermal input. Increasing thermal energy to PCM will accelerate its ability to change its phase, shorten the duration of time the PCM is charged, and result in an increase in liquid produced. When the input thermal energy supplied to the PCM exceeds the thermal energy required for the latent heat of the PCM, the operating temperature of the system will stay in the range of the phase change, or a temperature plateau will occur, and the temperature will not increase limitless, with latent heat of the PCM being the primary consumption of energy for use in the system (Avargani et al., 2021).

The matching of power input to the structural properties of the bed is considered an essential factor for achieving a uniform and rapid phase change. There is evidence in the literature that by optimizing solar power control, particle size and the porosity of the bed provide an opportunity for efficient heat transfer through the bed resulting in the liquid fraction having an almost complete phase change in a very short period. In a practical application of a district heating station, the improvement of solar power will affect both thermodynamic parameters as well as the consumption of energy by the system pumps and the overall operational cost and reliability (Avargani et al., 2021; Wu et al., 2024; Wu et al., 2026).

3 Methodology and Evaluation Framework

This chapter establishes a COMSOL-based numerical framework for analyzing temperature gradients, phase change propagation, and the coupled influence of key parameters in porous media packed-bed latent heat storage systems.

3.1 Structural Description of the Packed Bed Latent Heat Storage System

A latent heat storage system based on a porous medium packed bed is the subject of this study, which is made up of storage units and HTF circuits. Figure 5 shows that the bed contains phase-change material which is stored in a particle-like form, and the bed itself is treated as a homogeneous porous medium. In charging and discharging, the HTF flows axially through the packed bed under the influence of the external driving fluid and exchanges heat with the PCM particles.

The pack-style storage system transfers heat from HTFs to low-temperature PCMs, causing the phase change of the PCM. The storage system then recovers energy as the converted (solid) PCM returns to a liquid state during discharge to low-temperature. The system has a very compact form and gives a relatively large HTF-PCM thermal contact area, which qualifies it for use as a thermal energy storage system for medium and low-temperature applications.

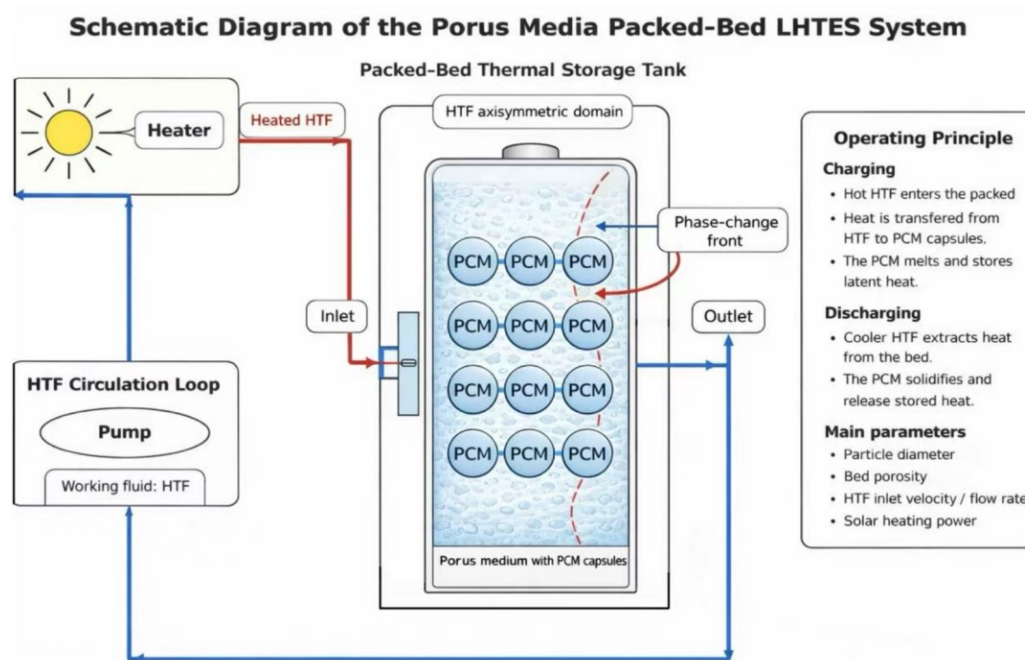


Figure 5. Schematic of the packed-bed latent heat thermal energy storage system

For simplified analysis, this study employs a two-dimensional axisymmetric model to describe the packed bed, assuming that PCM particles are uniformly distributed within the bed. The macroscopic heat transfer and flow behavior are treated as equivalent to those of a porous medium.

3.2 Basic Modeling Assumptions

To ensure the computability and reasonableness of the model, the following assumptions are made during the numerical modeling process:

PCM particles in the packed bed are uniform in size, and the bed porosity is spatially constant. The heat transfer fluid is considered incompressible Newtonian, and its physical properties are assumed constant within the calculation temperature range. Flow within the porous medium is treated as laminar flow. Radiation heat transfer is neglected, considering only convective and conductive heat transfer. PCM phase change occurs within a limited temperature range, which can be described using the enthalpy method, a formulation that incorporates both sensible and latent heat contributions while tracking phase change. Effects of PCM volume change and bed structure deformation are ignored.

These assumptions are widely adopted in numerical modeling studies of packed bed latent heat storage systems, ensuring computational accuracy while effectively reducing model complexity (Embale et al., 2025; He et al., 2022; Khattari et al., 2020).

3.3 Numerical Solution Method and Software Platform

This study employs COMSOL Multiphysics for numerical simulation. COMSOL has multi-physics coupling capabilities, effectively handling the strongly coupled problems among fluid flow, heat transfer, and phase change processes, making it suitable for the numerical modeling of packed bed latent heat storage systems .

During model implementation, fluid flow is described using a porosity-corrected laminar flow model for the porous medium. Energy transfer is calculated through a Local Thermal Non-Equilibrium (LTNE) model, which allows the fluid temperature

to respond faster than the solid phase, capturing the inherent delay of the solid matrix and PCM. The PCM phase change process is incorporated into the enthalpy formulation. The simulation is performed as a transient analysis to capture the dynamic response characteristics of the system during charging and discharging processes (Embiale et al., 2025; Khattari et al., 2020).

3.4 Geometric Model and Mesh Division

Based on the system's structural characteristics, this study establishes a two-dimensional axisymmetric geometric model to reduce computational cost while ensuring calculation accuracy. The geometric dimensions of the model are set according to a typical packed bed latent heat storage unit, with the bed region considered as a homogeneous porous medium.

For mesh generation, a free triangular mesh is used to discretize the computational domain. Local mesh refinement is applied at the fluid inlet, the bed region, and areas with large temperature gradients to improve the stability and accuracy of the numerical calculation. The overall number of mesh elements is reasonably controlled to ensure computational accuracy while maintaining computational efficiency.

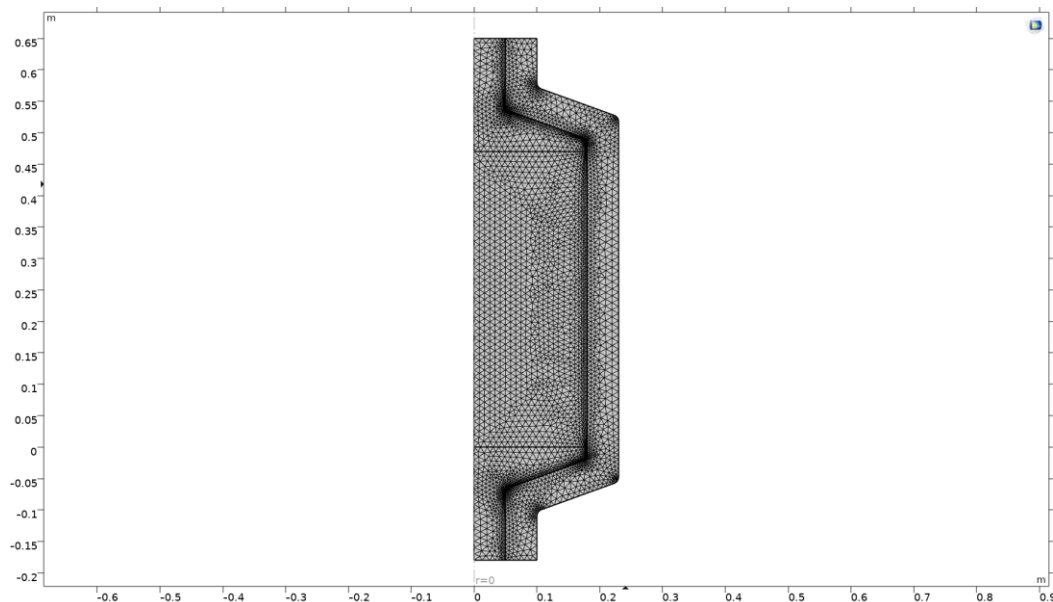


Figure 6. Mesh distribution of the packed-bed latent heat storage unit (COMSOL)

In the Figure 6, the computational mesh consists of a total of 7,594 elements, including 7,006 triangular elements and 588 quadrilateral elements. Local mesh

refinement is applied at the fluid inlet, the bed region, and areas with large temperature gradients to ensure numerical accuracy while maintaining computational efficiency (COMSOL, n.d.).

3.5 Initial Conditions and Model Setup

To simulate the actual operational conditions of the packed bed latent heat storage system, the model is set up with the following boundary conditions and initial conditions in Table 1 which is based on the COMSOL models 6.3 (COMSOL, n.d.):

Table 1. Initial Data

Name	Value	Description
dp	0.055 m	Diameter of PCM
por	0.49	Bed porosity
V(in)	3.33×10^{-5} V/s	Flow rate
T0	305.15 K	Initial temperature
Qu	375W	Solar heating power
Rho(av)	819.5 kg/m ³	Average density

4 Results and Discussion

Here we present the primary findings of our work, addressing how both particle diameter and porosity impact the ability of a packed-bed thermal energy storage system to charge. To assist with design improvements that can maximize efficiency, we have also reviewed the tendencies exhibited in the simulation results.

4.1 Baseline Data Results

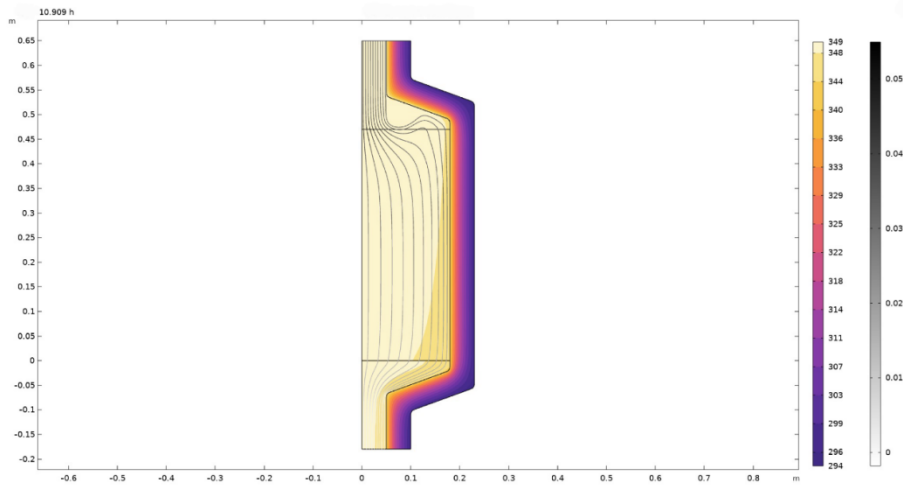


Figure 7. Isotherms (ht) and velocity streamlines (COMSOL)

Figure 7 shows that it takes about 10.9 hours to fully charge the porous media and complete the operation of the packed bed.

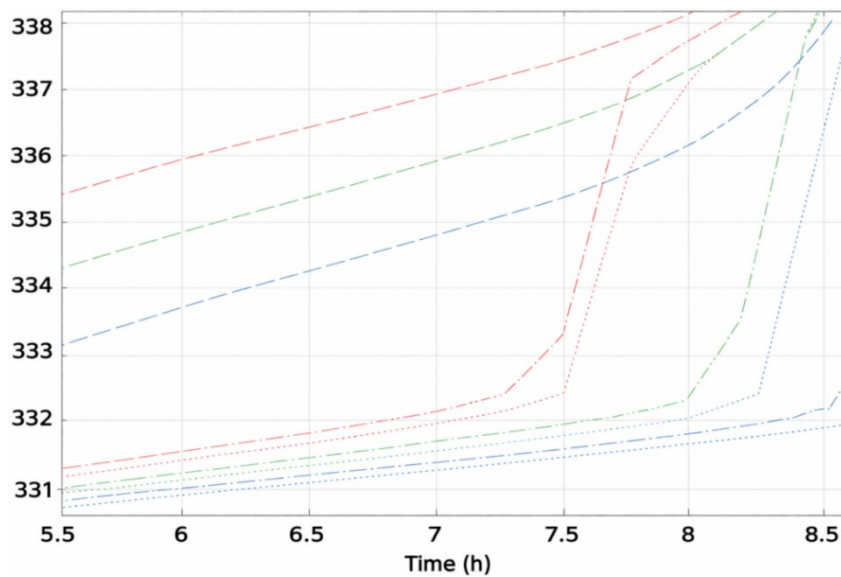


Figure 8. Temperature evolution (COMSOL)

Figure 8 illustrates the temperature evolution at different points within the packed bed for paraffin, water, and the porous media. For paraffin, the temperatures at positions 0.05 m, 0.235 m, and 0.42 m are represented by blue, green, and red dotted lines, respectively. For water, the corresponding positions are indicated by blue, green, and red dashed lines. The porous media temperatures at these positions are shown using blue, green, and red dash-dot lines. This figure captures the spatial variation in temperature and highlights the differences in heating rates among the three materials during the charging process.

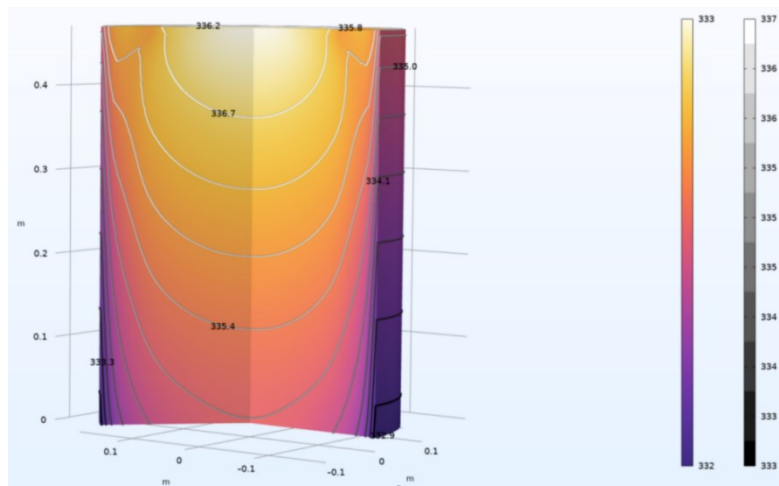


Figure 9. Material temperature (K) isotherms and fluid temperature (K) (COMSOL)

The thermal profile of the packed-bed packing medium and fluid, as shown in Figure 9, demonstrates how temperature varies in three-dimensional space. As shown by the isotherms, there is spatial disparity in the rate at which various regions of the packed bed material heat up (charging) throughout all of the time periods studied.

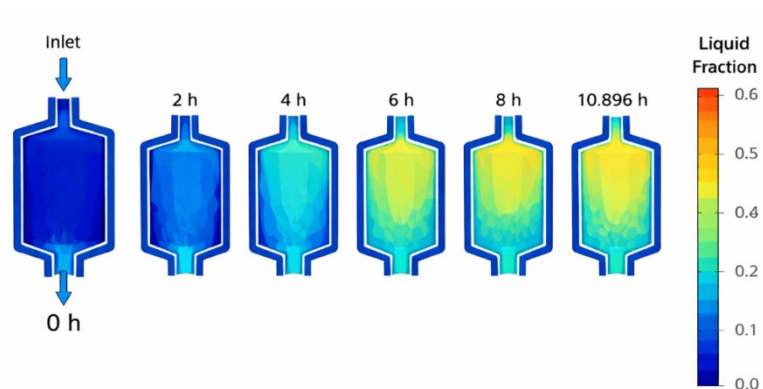


Figure 10. Liquid fraction distribution (COMSOL)

The images shown in Figure 10 show how the liquid fraction of the phase change material (PCM) has changed over the period. The series of images illustrate how melting occurs as the PCM travels from its inlet position into the downstream regions, showing the system being charged with energy.

4.1.1 Volumetric Heat Storage Density

The volumetric heat storage density of a porous media storage system refers to the maximum effective heat that can be stored per unit volume of the porous medium structure. It is a key metric to quantify the compactness of the storage system and its storage capacity, directly reflecting the energy storage capability within a limited volume.

The following parameters need to be obtained before calculation in Table 2 (from experimental measurements or numerical simulations, e.g., COMSOL):

Table 2. Needed Data Before Calculation

Physical Meaning	Symbol	Unit	Initial Data / Value
Total Bed Volume	V _(bed)	m ³	0.046
Total PCM Mass	m(PCM)	kg	21.21
PCM Latent Heat	L	J/kg	200,000
PCM Sensible Heat Temperature Difference	ΔT	K	42.85
PCM Specific Heat	C _p (PCM)	J/(kg·K)	2000
PCM Average Liquid Fraction	f(liq)	–	0.6
Charging Time	t	h	10.9

The total volume of the packed bed can be calculated using equation:

$$V_{\text{bed}} = \pi r^2 h \quad (1)$$

Given:

$r=0.18\text{m}$, $h=0.46\text{m}$

The total Mass of PCM can be calculated using equation:

$$m_{\text{PCM}} = \rho_{\text{PCM}} \times V_{\text{bed}} \times (1 - \text{por}) \quad (2)$$

Total Thermal Energy can be calculated using equation:

$$Q_{\text{stored}} = m_{\text{PCM}} \times [c_{p,\text{PCM}} \times \Delta T + L \times f_{\text{liq}}] \quad (3)$$

Volumetric Heat Storage Density (Sensible Heat + Latent Heat) can be calculated using equation:

$$\rho_V = \frac{Q_{\text{stored}}}{V_{\text{bed}}} \quad (4)$$

If only latent heat is considered, the volumetric heat storage density can be calculated using equation:

$$\rho_V(\text{latent heat}) = \frac{m_{\text{PCM}} \times L \times f_{\text{liq}}}{V_{\text{bed}}} \quad (5)$$

Volumetric Heat Storage Density (Sensible + Latent Heat): 87.3 MJ/m^3

4.1.2 Volumetric Heat Storage Power

The volumetric heat storage power of a porous media storage system is defined as the effective power per unit volume of the porous medium structure during the charging/discharging process. It reflects the power density and dynamic response characteristics of the system and serves as a key indicator for evaluating the compactness and time efficiency of the storage system.

The volumetric heat storage power (based on stored heat and charging time) is calculated as:

$$P_V = \frac{Q_{\text{stored}}}{V_{\text{bed}} \times t} \quad (6)$$

Where, the formula for total stored heat is:

$$Q_{\text{stored}} = m_{\text{PCM}} \times [c_{p,\text{PCM}} \times \Delta T + L \times f_{\text{liq}}] \quad (7)$$

Volumetric Heat Storage Power: 2407 W/m³

4.2 Improvement-Oriented Analysis

In practical operation, Figure 11 shows that the adjustable range of particle diameter d_p is approximately 5–75 mm. At the same time, the best data group could be found in Figure 11 ($d_p = 5$ mm and $\text{por} = 0.6$, the charging time is 9.5 h), because of the shortest charging time.

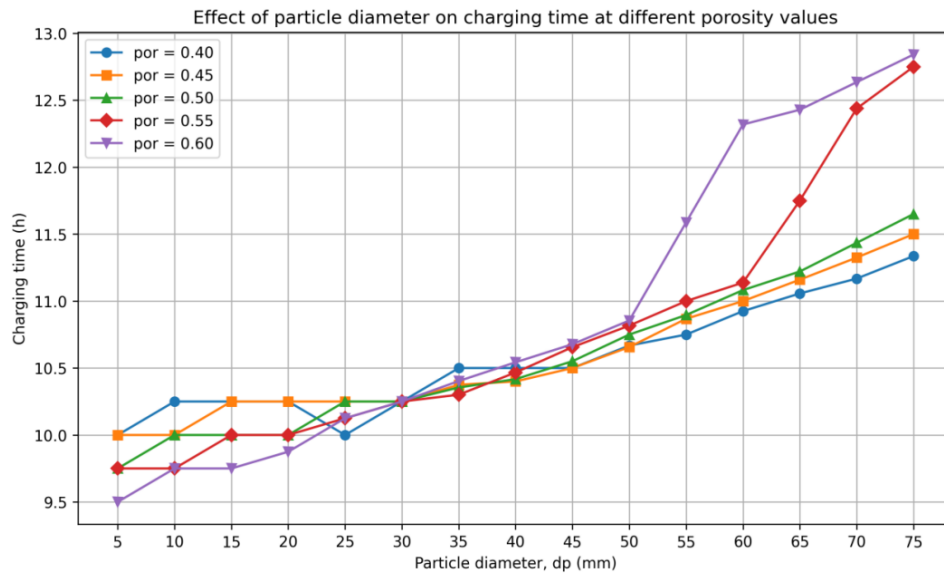


Figure 11. Charging Time focused on d_p and por

In the focused study on “ d_p – porosity – charging time”, the influence of particle diameter and porosity on charging time is not independent, but forms a positive and negative feedback relationship through the “heat transfer efficiency”, which can be analyzed by combining theoretical assumptions and experimental data as follows:

4.2.1 Theoretical Hypothesis

In the packed bed charging procedure, multiple associated mechanisms occur: (1) Fluid heat transfer; (2) Heat transfer through the pore channels; and (3) Heat stored in the PCM particles' structure. The particle diameter and porosity of the packed bed both impact this overall charging process.

Larger particles have more thermal resistance than smaller particles, allowing heat to penetrate more readily into the PCM particle. Porosity affects the charging process in two ways: first, with increasing porosity, there is less flow resistance, which may improve the distribution of HTF flow, and second, there will be less total PCM available because the larger amount of porosity will take up some of the volume of the PCM bed. Therefore, it cannot be said that the increased rate of charging due to higher porosity is only due to improved flow conditions, but rather that there is a reduction of total PCM mass present in the system.

Conversely, when porosity decreases, the PCM content in the bed increases, which can enhance total storage capacity but also requires more energy and time to complete the charging process. Therefore, the influence of porosity on charging time should be understood as the combined effect of flow resistance, heat transfer conditions, and the total PCM mass contained in the packed bed.

4.2.2 Actual Data Analysis

The best data group ($d_p = 5$ mm and $por = 0.6$, the charging time is 9.5 h) which is obtained in Figure 11 validate the above hypothesis. A small particle diameter combined with high porosity forms a positive feedback case and gives the shortest charging time. For example, at $d_p = 5$ mm and $por = 0.6$, the charging time is 9.5 h, the shortest among all cases, because the smaller diameter reduces thermal resistance and the higher porosity reduces flow resistance, so heat transfer is enhanced. Additionally, the decrease in PCM mass also contributes to a shorter charging time. In contrast, a large particle diameter combined with low porosity forms a negative feedback case and leads to a longer charging time. At $d_p = 75$ mm and $por = 0.4$, the charging time increases to 11.336 h, about 19% longer than the case of $d_p = 5$ mm and $por = 0.6$, because both thermal resistance and flow resistance increase. A

compensatory feedback case appears when both diameter and porosity increase at the same time. When d_p increases from 5 mm to 20 mm and por increases from 0.4 to 0.6, the charging time changes only slightly from 10 h to 9.875 h, showing that the increase in thermal resistance is offset by the decrease in flow resistance, so the charging time remains nearly stable.

4.2.3 Improvement of Volumetric Heat Storage Density

To increase the volumetric heat storage density of the porous media storage system, the core idea is to maximize the effective stored heat per unit volume while keeping the total volume of the packed bed unchanged. The best group is set in the Table 3.

Increasing the volumetric heat storage density in a packed bed by decreasing the porosity of the packed bed results in an increase in the volume fraction of PCM and mass of PCM for the same bed volume. In the previous example, the porosity was reduced from 0.49 to 0.40 and this reduction is acceptable. However, if the porosity is reduced below 0.40, the resistance to flow will likely become excessively high and the charging time may increase significantly.

By raising the final liquid fraction, the storage density will also increase as more of the PCM will finish changing phase and thus contribute latent heat. For example, the liquid fraction can be increased from 0.6 to 0.95 by either improving the heating power or extending the charge time, and without the risk of overheating in any area.

Expanding the sensible heat temperature difference can further increase the total stored heat. Increasing $\Delta T = T(\text{end}) - T(\text{start})$, such as by raising the final charging temperature, allows more sensible heat to be stored. However, the final temperature must remain below the decomposition temperature of the PCM.

If the porosity is less than 0.4: Flow resistance in the bed increases sharply, leading to higher pump/fan power consumption, and may even cause uneven fluid distribution and local “dead zones”. Charging time significantly increases, reducing the effective utilization of solar energy and causing additional heat loss due to prolonged heat transfer. Excessively high particle packing density may limit the volumetric expansion of PCM during phase change, posing structural stress risks to the bed.

Therefore, the final selected porosity is 0.4.

Table 3. Selected combination of Solar Power and Dp-Por

Solar Power (W)	Full Charging Time (h)	Dp Particle Diameter(mm)	Por Porosity	Liquid Fraction
400	9.5	5	0.4	0.8
450	8.25			0.9
500	7.5			0.9
550	6.75			0.95
600	6.17			1

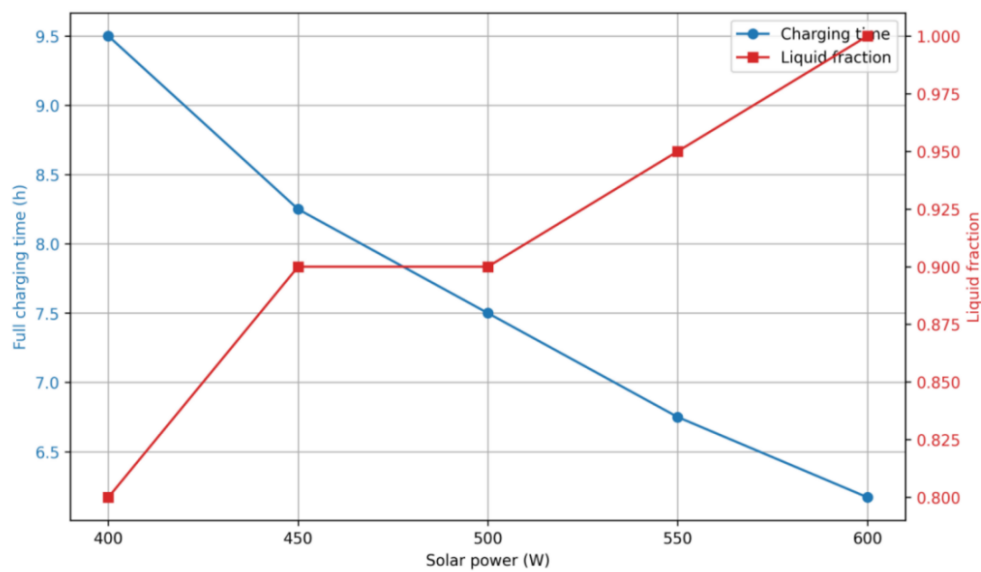


Figure 12. solar power-charging time

In the Figure 12, Considering the practical collector power limit of about 700–800 W/m², the solar heating power was increased from 375 W to 600 W. Combined with a 5 mm PCM particle diameter, this provides faster heat transfer and shorter charging time without exceeding the practical system limit.

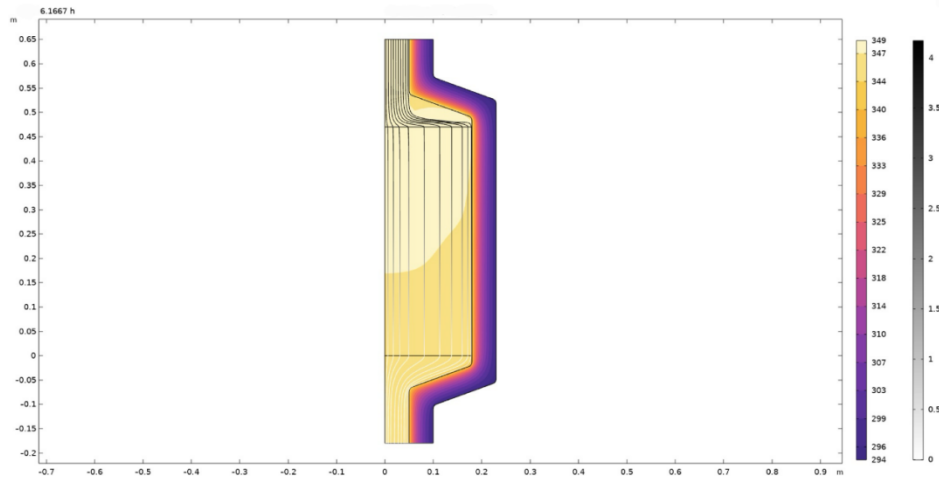


Figure 13 Isotherms (ht) and velocity streamlines (COMSOL)

In the Figure 13 the temperature field at about 6.2 h confirms the effectiveness of the improved condition. The charging time decreases markedly, the bed temperature gradient remains small, and the streamlines stay evenly distributed, indicating that the higher power input improves heat transfer without causing severe local overheating.

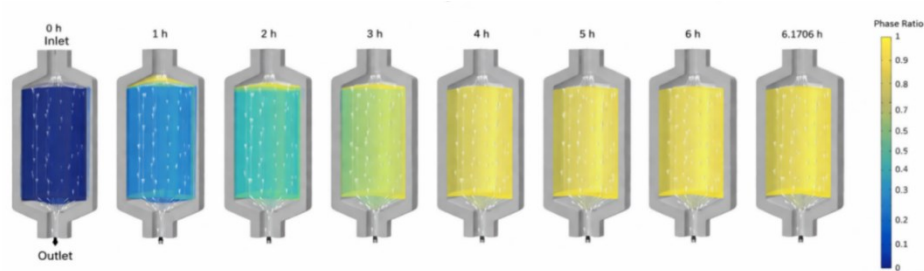


Figure 14. Liquid fraction evolution (COMSOL)

The liquid-fraction distribution under the optimized combination of 600 W, 5 mm particles, and about 6.2 h charging time is close to complete melting over most of the bed, Figure 14 showing that coordinated improvement can substantially improve phase change completion.

4.2.4 Expansion of the Sensible Heat Temperature Difference

The material properties determine the theoretical upper limit of the final heating temperature and the phase change temperature range. The key parameters include:

Phase change temperature: For the same PCM (such as paraffin), the solid–liquid phase change temperature is fixed (for example, 58–62 °C). During the phase change process, even if heating continues, the material temperature remains near the phase change temperature until it is completely melted into the liquid state (Avargani et al., 2021, Wang, 2025).

Thermal decomposition temperature: Every PCM has its thermal stability limit. If the heating temperature exceeds this value, the material will decompose and carbonize, losing its heat storage capability. This is the absolute upper limit of the final heating temperature (Wang, 2025).

Under the above conditions, the final charging temperature data obtained from COMSOL are shown in Table 4:

Table 4. Final charging temperature data

Dp Particle Diameter (mm)	Por Porosity	Solar Heating Power (W)	Final Fully Charged PCM Temperature (°C)
5	0.4	375	74.85
		400	74.85
		450	74.85
		500	74.85
		550	74.85
		600	74.85

Within this allowable range, heating power, charging duration, heat-transfer conditions, and system heat loss jointly determine the actual final temperature. In the present model, increasing solar power accelerates the approach to the melting region but does not further increase the final PCM temperature once the critical melting temperature is reached.

4.2.5 Updated Volumetric Heat Storage Density Results

Total PCM mass can be calculated using equation, m_{PCM} (when porosity = 0.4):

$$m_{\text{PCM}} = \rho_{\text{PCM}} \times V_{\text{bcd}} \times (1 - \text{por}) \quad (8)$$

Where the liquid fraction $f(\text{liq}) = 1$

Volumetric Heat Storage Density (Sensible Heat + Latent Heat) is calculated as:

$$\rho_V \approx 154.3 \text{ MJ/m}^3$$

Table 5. Independent Variables

Comparison Indicator (Variable)	Initial Case	improved Case	Change
Porosity (por)	0.49	0.4	Decreased by 18.4%
Diameter (dp)	55	5	Decreased by 90.91%
Solar Power	375	600	Increased by 160%

Table 6. Dependent Variables

Other Dependent Variable	Initial	Optimized	Change
Total PCM Mass (kg)	21.21	24.95	Increased by 17.6%
Liquid Fraction $f(\text{liq})$	0.6	1	Increased by 66.7%
Charging Time (h)	10.9	6.2	Reduced by 56.63%
Volumetric Heat Storage Density (MJ/m^3)	87.3	154.3	Increased by 176.7%

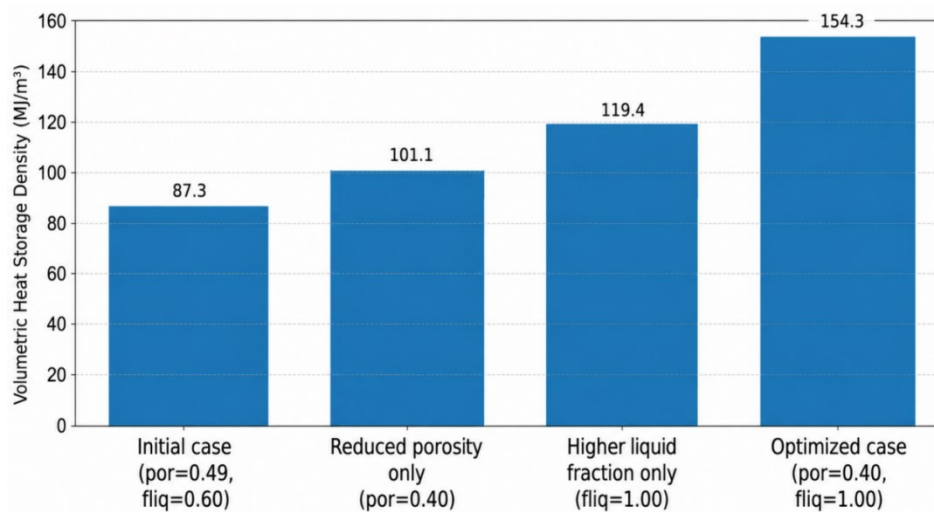


Figure 15. Effect of key improvement factors on volumetric heat storage density

In the Table 5, the paraffin-based porous media packed-bed system reducing porosity from 0.49 to 0.40 and increasing the liquid fraction from 0.6 to 1 significantly improved volumetric heat storage density. The total value rose from 87.3 MJ/m³ to 154.3 MJ/m³, according to the Table 6 and Figure 15, showing that higher PCM filling and more complete phase change are effective ways to improve storage compactness.

4.2.6 Improvement of Volumetric Heat Storage Power

To improve volumetric heat storage power, the system must shorten charging time while maintaining sufficient stored heat. This requires balancing heat-transfer enhancement and storage capacity.

Core Idea: Shorten the Charging Time (Priority) + Ensure Effective Heat Storage Capacity.

The formula for volumetric heat storage power is

$$P_V = \frac{Q_{\text{effective}}}{V_{\text{bed}} \cdot t_{\text{charge}}} \quad (9)$$

To improve the volumetric heat storage power, charging time must be made as low as possible while not adversely affecting effective heat stored amounts. Data suggest that combining high porosity and small particle diameter will typically result in a shorter period of time required to charge these materials. For example, the time period required to charge material with $d_p = 5$ mm and $\text{por} = 0.6$ is 9.5 h. Conversely, material with $d_p = 20$ mm and $\text{por} = 0.4$ will take 10.9 h. Therefore, for these materials, reducing d_p from 20 mm to 5 mm, while simultaneously increasing por from 0.4 to 0.6, reduces the total time for charging by approximately 7.3%. Another means of reducing time needed to charge material can be achieved through increasing heating power. An apparent efficiency increase occurs when the solar heat input increases from 400 to 800 W. In this case, the total charging time decreased from 9.5 hours to 4.6 hours, and at the same time, the liquid fraction increased to 1, thus enhancing the effective heat storage. The overall findings indicate that a strategy

consisting of smaller particle sizes, higher porosities, and higher heat inputs results in shorter charging times, while maintaining or enhancing storage performance.

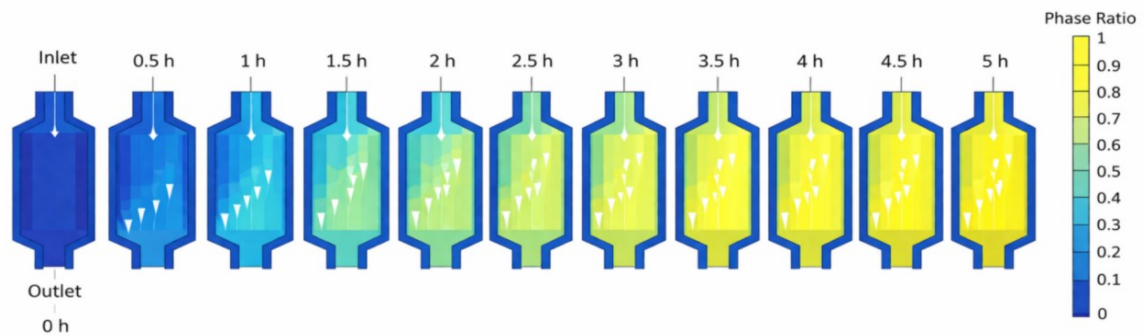


Figure 16. Liquid fraction evolution (COMSOL)

Figure 16 shows that a higher power input can accelerate the rate of heat transfer to the PCM, thereby directly shortening the charging time.

4.2.7 Improved Data

Table 7 Independent Variables(por-dp-power)

Comparison Indicator (Variable)	Initial Case	Improved Case	Change
Porosity (por)	0.49	0.4	Decreased by 18.4%
Diameter (dp)	55	5	Decreased by 90.91%
Solar Power	375	800	Increased by 213.3%

Table 8 Dependent Variables(mass-Liquid Fraction-Charging Time)

Other Dependent Variable	Initial	Optimized	Change
Total PCM Mass (kg)	21.21	24.95	Increased by 17.6%
Liquid Fraction	0.6	1	Increased by 66.7%

Charging Time (h)	10.9	4.6	Reduced by 42.4%
Volumetric Heat Storage Power (W/m ³)	2407	9283	Increased by 285.7%

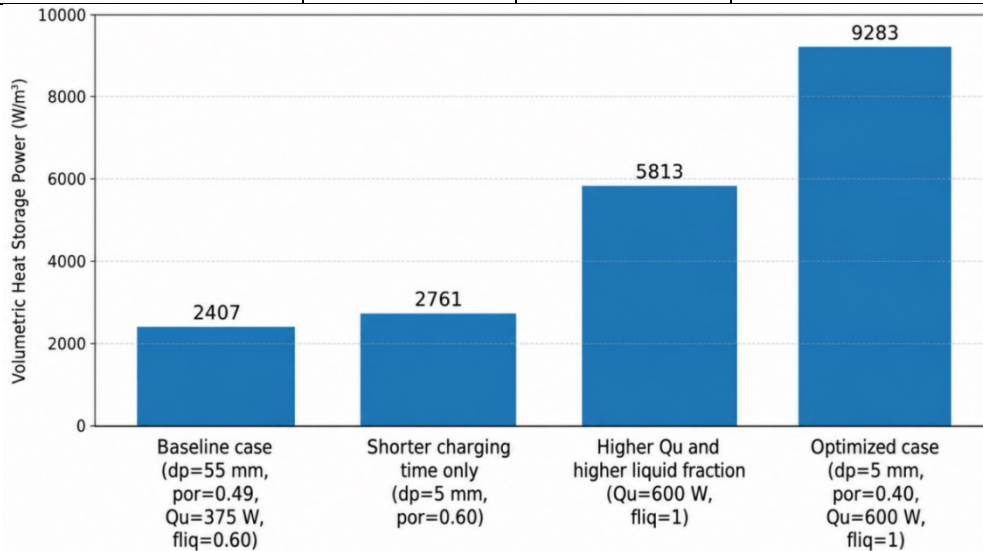


Figure 17. Effect of key improvement factors on volumetric heat storage power

In table 7, they show a significant improvement in volumetric heat storage power was achieved by improving the key parameters of the porous media thermal storage system. Specifically, the particle diameter was set to 5 mm, and the porosity was reduced from 0.49 to 0.4, which increased the total PCM mass by 17.6%. At the same time, according to table 8, and figure 17 the liquid fraction was increased from 0.6 to 1 to fully release the latent heat of phase change, and the heating time was shortened from 10.9 h to 6.2 h through improvement of the solar heating power, representing a reduction of 43.5%.

After multi-parameter coordinated improvement, the volumetric heat storage power of the system increased from the initial 2407 W/m³ to 9283 W/m³, with an improvement of 189.1%. This result demonstrates the effectiveness of the improvement path of “reducing porosity to enhance heat storage capacity + shortening heating time to improve heat storage rate.”

4.3 Influence of Particle Diameter and Porosity

To reveal the influence law of structural parameters on dynamic response, this study carried out a combination scan for dp (5–75 mm) and por (0.40–0.60). The results

show that the charging time generally falls within the range of about 9.5–12.8 h. Among them, smaller d_p corresponds to shorter charging time under most porosity conditions, while larger d_p often leads to an increase in charging time. The shortest charging time appears at $d_p=5$ mm, $\text{por}=0.60$ (about 9.5 h), whereas in the large-diameter range (such as $d_p=75$ mm), the charging time becomes significantly longer. In general, smaller particle diameters (d_p) provide shorter charging times at most porosity levels because there is more surface area, which means heat is transferred more rapidly between the fluid and the packed bed. On the other hand, larger particle diameters have longer charging times primarily because there is less surface area for heat to be exchanged with the packing.

Reconstructed dynamic responses under different particle diameters ($\text{por} = 0.40$)

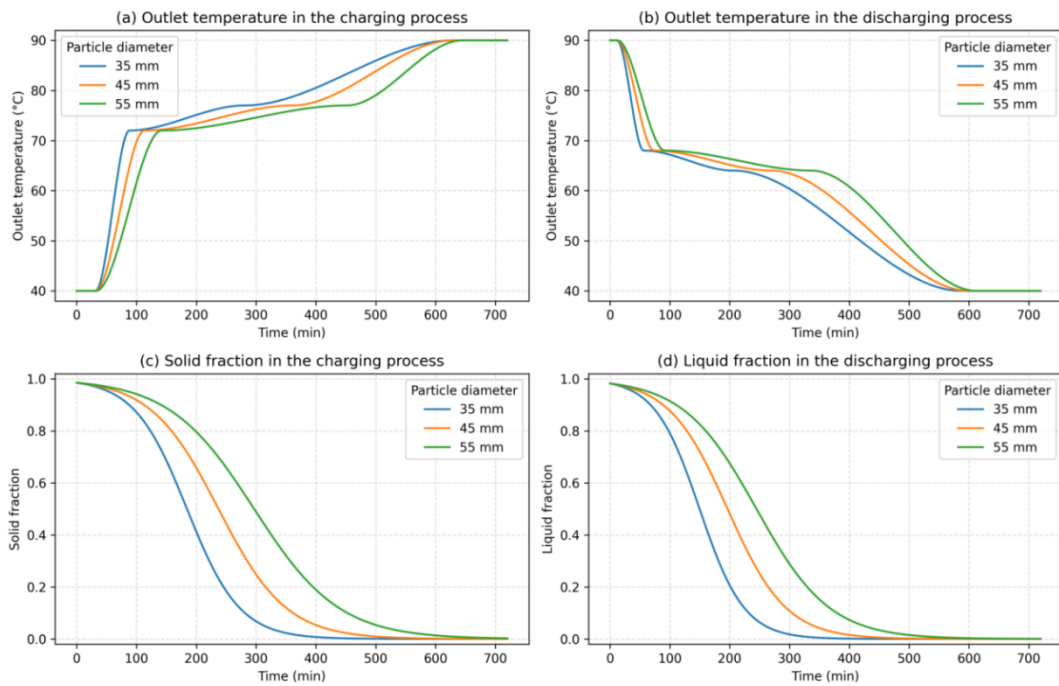


Figure 18. Reconstructed dynamic responses of outlet temperature and phase fraction during charging and discharging under different particle diameters.

The dynamic response figure 18 further clarify the physical meaning of the structural improvement results. The group of curves under different particle diameters shows that smaller particles lead to a faster rise in outlet temperature during charging, a faster decline in solid fraction, and a more rapid decrease in liquid fraction during discharging. This means that reducing particle diameter enhances both the charging

and discharging response rates. In contrast, larger particles produce a slower propagation of the thermal front and a more delayed phase change process because of the larger internal thermal resistance.

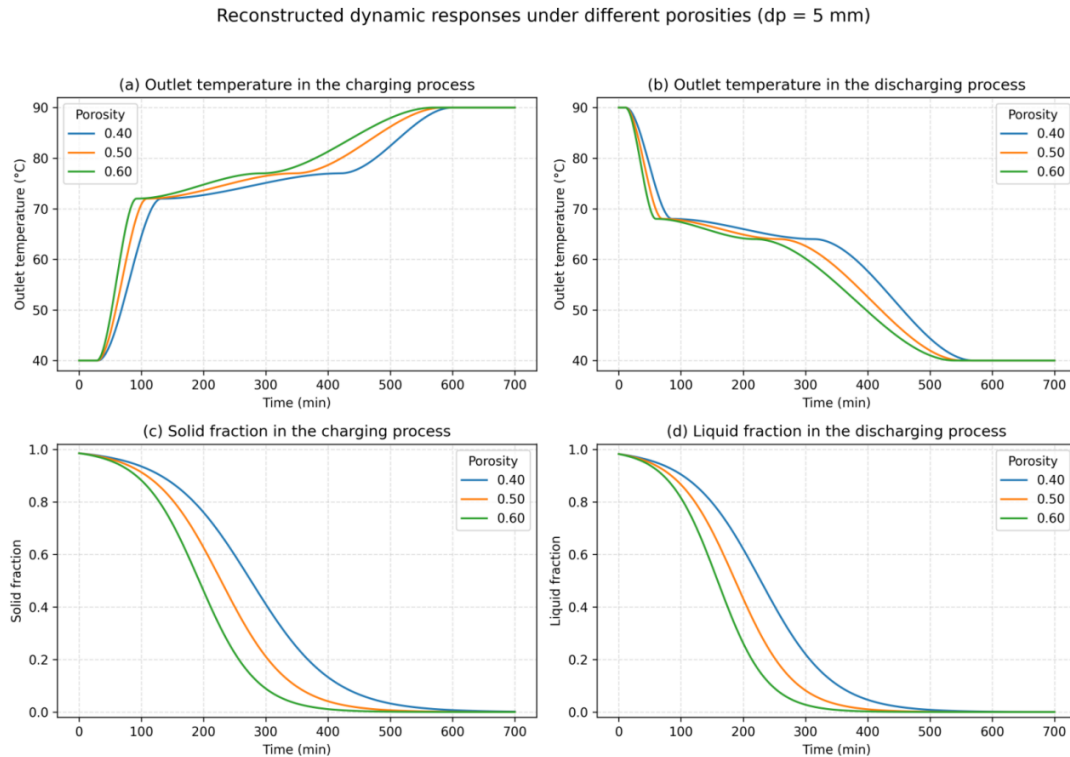


Figure 19. Reconstructed dynamic responses of outlet temperature and phase fraction during charging and discharging under different porosities.

In the Figure 19, the curves under different porosities show that a larger porosity generally improves the fluid passage and accelerates the thermal response, especially in the early and middle stages of charging and discharging. However, porosity does not only affect the rate performance. Increasing porosity also reduces the effective PCM filling amount in the same bed volume, which may weaken the storage compactness. Therefore, the results confirm that porosity must be optimized by balancing heat transfer enhancement and storage-capacity retention rather than by simply maximizing the void fraction.

It should also be pointed out that real packed beds may be affected by the wall effect, which can induce radial porosity fluctuations and thereby alter local flow and heat transfer distribution. This is also a potential source of error for the two-dimensional uniform porous-medium equivalent model. Related studies have shown that the radial

porosity oscillation caused by wall effects can influence the flow and heat transfer behavior of packed-bed PCM systems.

5 Pressure loss assessment

To ensure that the comprehensive improvement scheme proposed in this study not only has advantages in heat transfer and phase change performance, but is also feasible at the engineering operation level, the pressure drop ΔP of the packed bed is introduced as an engineering cost indicator to independently assess the improvement results. The validation idea is as follows: under the same bed geometry and the same flow-rate operating condition, the Ergun correlation is used to calculate the pressure drop of each scheme, and the engineering rule of thumb that “the pressure drop should not exceed 20% of the inlet pressure” is taken as the constraint criterion to determine whether the improvement scheme meets the requirements of engineering operability.

5.1 Definition of Pressure Drop and Validation Criterion

The pressure drop of the packed bed is defined as the average static pressure difference between the bed inlet and outlet:

$$\Delta P = P_{in} - P_{out} \quad (10)$$

In porous media packed beds and chemical reactors, taking the inlet pressure as 5 atm or several times atmospheric pressure is a commonly used rule of thumb in engineering design (Georgousis et al., 2025; Wu et al., 2026). This is adopted to ensure that the pressure-drop calculation is consistent with actual operation, while also satisfying the requirements of fluid-dynamic stability.

$$P_{in,abs} = P_{atm} = 506625 \text{ (Pa)}$$

The engineering criterion is:

$$\Delta P \leq 0.2 P_{in,abs}$$

Maximum allowable pressure drop:

$$\Delta P_{\max}=101325 \text{ Pa}$$

5.2 Pressure Drop Calculation Model (Ergun Equation)

The pressure drop of the packed bed is estimated using the classical Ergun correlation, which can characterize the sensitivity of pressure drop to porosity, particle diameter, and superficial velocity: (Georgousis et al., 2025; Zhou, 2025)

$$\frac{\Delta P}{L} = \frac{150\mu(1-\varepsilon)^2}{\varepsilon^3 d_p^2} u + \frac{1.75\rho(1-\varepsilon)}{\varepsilon^3 d_p} u^2 \quad (11)$$

Where ε is the porosity (por), d_p is the particle diameter, L is the effective bed length, μ and ρ are the dynamic viscosity and density of the fluid, respectively, and u is the superficial velocity. The superficial velocity is calculated as:

$$u = \frac{\dot{V}}{A} \quad (12)$$

where \dot{V} is the volumetric flow rate, and A is the cross-sectional area of the bed.

5.3 Parameter Substitution and Calculation Process

(1) The volumetric flow rate \dot{V} can be calculated as follows. In this study, all cases adopt the same inlet flow rate of 2 L/min

$$\dot{V} = uA = 3.333 \times 10^{-5} \text{ m}^3$$

(2) Bed geometry basis can be calculated using equation:

Consistent with the calculation basis used in this study for volumetric heat storage density, the effective bed volume is taken as $V_{bed} \approx 0.05$, and the effective height is $L=0.47\text{m}$. Therefore, the cross-sectional area is

$$A = \frac{V_{bed}}{L} = 0.1064 \text{ m}^2 \quad (13)$$

(3) Superficial velocity can be calculated using equation:

$$u = \frac{\dot{V}}{A} = 3.13 \times 10^{-4} \text{ m/s} \quad (14)$$

The operating temperature range of the system is approximately 305–348 K. For order-of-magnitude estimation, average fluid properties are adopted in this study:

$$\mu = 6.0 \times 10^{-4} \text{ Pa}\cdot\text{s} \quad \rho = 990 \text{ kg/m}^3$$

5.4 Pressure Drop Results and Table Summary

Table 9. Pressure Drop Calculation Results

Scheme	(por)	dp	ΔP (Pa)	Allowable Upper Limit (Pa)	ΔP
Baseline case	0.49	55	0.016	101325	3.16×10^{-8}
Comprehensive optimized case	0.4	5	3.132	101325	6.18×10^{-6}
Fast-charging optimized case	0.4	5	3.132	101325	6.18×10^{-6}

Compared with the baseline case, in Table 9, the pressure drop of the comprehensive improved case and the fast-charging case increases significantly (0.016 Pa \rightarrow 3.132 Pa), which is consistent with the trend predicted by the Ergun equation. When the particle diameter decreases from 55 mm to 5 mm, the viscous term is sensitive to particle diameter at the order of $\frac{1}{d_p^2}$, so the pressure drop increases significantly. At the same time, when the porosity decreases from 0.49 to 0.40, the $\frac{1}{\varepsilon^3}$ term increases, which further raises the pressure drop. Therefore, the direction of pressure-drop increase is fully consistent with the physical mechanism, indicating that the improvement scheme does not exhibit any non-physical abnormality in terms of flow resistance (Georgousis et al., 2025; Zhou, 2025).

Therefore, from an engineering perspective, although the comprehensive improved case increases the pressure drop, the increase remains negligible under the current

flow rate and device size and does not limit operation. The observed trend that pressure drop increases as particle diameter decreases and porosity decreases is also consistent with the Ergun equation, confirming that the proposed improvement is reasonable and practical. Since the fast-charging case and the comprehensive optimized case have the same flow parameters, changing the heating power Q does not affect the pressure drop, which is mainly governed by geometry and flow conditions.

5.5 Discussion of Limitations and Uncertainties

Certain uncertainties exist in the improved intermediary configurations related to changing materials, manufacturing tolerances, and idealized simulated conditions, just as with traditional state-of-the-art packed bed PCM systems. The use of small particle size (5 mm) and greater porosity (0.60) allows the system to produce a quicker thermal response and improved effective heat capacity than its state-of-the-art packed bed PCM equivalent, while still yielding reasonable pressure drop values. As a follow-up effort, experimental validation of these results is suggested in order to confirm real-world viability.

6 Conclusion

This study numerically investigated the charging performance of a porous media packed-bed latent heat thermal energy storage system under baseline and improved conditions.

As indicated in the baseline condition, this system has a typical packed-bed charging process in which the thermal front propagates from the inlet to the downstream. The results also exhibit fluid-solid temperature mismatches under LTNE, indicating a faster response of the fluid relative to the solid phase in the charging process. The liquid fraction distribution also indicates that there is spatial non-uniformity in phase change propagation; additionally, the regions nearest to the inlet melted before the downstream and edge regions.

Improvement of charge performance has resulted from optimizing the process parameters. Specifically, decreasing particle size, selecting an adequate porosity, and increasing solar heating power have facilitated more uniform phase change propagation over the entire charged portion of the material, leading to a shorter charge time. With the increase in solar heating power from 400 W to 600 W, the time required to achieve a full charge decreased from approximately 9.5 hours to 6.1706 hours, and the percentage of liquid at the end of charging increased from approximately 80% to 100%. Increasing solar heating power to roughly 800 W would further reduce charge time to approximately 4.619 hours, although for engineering reasons, increasing to 600 W ($Q_u = 600$ W) is considered a better option.

Volumetric heat storage density increased from 87.3 MJ/mm³ to 154.3 MJ/m³, and volumetric heat storage power was increased from 2407 W/m³ to 9283 W/m³. improved system reduced porosity from 0.49 to 0.40, reduced particle size from 55 mm to 5 mm, Increased liquid fraction from 0.6 to 1, and reduced charging time from 10.896 hours to 6.1706 hours compared with the baseline case.

Table 10 Comparison of Key Parameter Combinations and Performance

Scheme	por	dp (mm)	Qu (W)	F(liq)	t (h)	Volumetric Heat Storage Power P(v) (W/m ³)	Volumetric Heat Storage Density (MJ/m ³)
Base case	0.49	55	375	0.6	10.896	2407	87.3
Improved case 1	0.4	5	600	1	6.1706	9283	—
Improved case 2	0.4	5	800	1	4.6169	—	154.3

Overall, the Table 10 shows that coordinated improvement of particle diameter, porosity, heating power, and phase change completion can effectively improve both storage compactness and dynamic charging performance. At the same time, future design should also consider the trade-off between thermal performance and pressure drop to ensure engineering feasibility.

7 References

Avargani, V.M., Norton, B., Rahimi, A. and Karimi, H. (2021) 'Integrating paraffin phase change material in the storage tank of a solar water heater to maintain a consistent hot water output temperature', *Sustainable Energy Technologies and Assessments*, 47, 101350.

Bentivoglio, F., Rouge, S., Soriano, O. and Tempass de Sousa, A. (2021) 'Design and operation of a 180 kWh PCM heat storage at the Flaubert substation of the Grenoble urban heating network', *Applied Thermal Engineering*, 185, 116402.

Chen, X., Zhang, J., Zou, H., Zhang, G., Zhang, A., Dong, Y., Liang, H. and Wang, F. (2024) 'Enhancing performance in heat storage unit and packed-bed system: Novel capsule designs inspired by drop structure', *Energy*, 313, 134047.

David-Hernández, M.A., Calderon-Vásquez, I., Battisti, F.G., Cardemil, J.M. and Cazorla-Marín, A. (2024) 'Design and assessment of a concentrating solar thermal system for industrial process heat with a copper slag packed-bed thermal energy storage', *Applied Energy*, 376, 124280.

Embiale, D.T., Padmanabhan, S.B., Mabrouk, M.T., Grieu, S. and Lacarrière, B. (2025) 'Neural-accelerated numerical model for packed bed latent heat storage system', *Energy and AI*, 22, 100602.

Georgousis, N., Diriken, J., Speetjens, M. and Rindt, C. (2025) 'Comprehensive review on packed-bed sensible heat storage systems', *Journal of Energy Storage*, 121, 116516.

He, X., Qiu, J., Wang, W., Hou, Y., Ayyub, M. and Shuai, Y. (2022) 'A review on numerical simulation, optimization design and applications of packed-bed latent thermal energy storage system with spherical capsules', *Journal of Energy Storage*, 51, 104555.

Hlimi, M., Lebrouhi, B.E., Belcaid, A., Lamrani, B., Balli, L., Ndukwu, M.C., El Rhafiki, T. and Kousksou, T. (2023) 'A numerical assessment of a latent heat storage system for district heating substations', *Journal of Energy Storage*, 57, 106210.

Khattari, Y., El-Otmany, H., El Rhafiki, T., Kousksou, T., Ahmed, A. and Ben Ghoulam, E. (2020) 'Physical models to evaluate the performance of impure phase change material dispersed in building materials', *Journal of Energy Storage*, 31, 101661.

Karthikeyan, S., Velraj, R. and Senthil, R. (2024) 'Overview of numerical, experimental and parametric studies on the spherical container-based packed bed latent heat storage', *Journal of Energy Storage*, 102, 114089.

Liu, S., Zhang, C. and Wu, Y. (2026) 'Numerical determination of volumetric heat transfer coefficient in packed bed thermal energy storage system considering gravity and flow orientation', *International Communications in Heat and Mass Transfer*, 172, 110211.

Wang, J. (2025) Study on the Heat Storage Performance of Waste Ore-based Composite Phase Change Material Filled Beds. Master's thesis.

Wei, H., Wei, Z., Zhu, H., Zheng, C., Li, B., Zhao, B. and Zhai, X. (2026) 'Experimental investigation and performance evaluation of direct contact phase change packed bed heat exchanger based on shape-stable phase change thermal storage unit', *Renewable Energy*, 257, 124760.

Wu, F., Cao, S., Qi, C., Sun, C. and Wu, X. (2024) 'Design and evaluation of a PCM heat accumulator applied in heating substations to accommodate supply-demand mismatch in district heating system', *Journal of Energy Storage*, 91, 111973.

Wu, F., Cao, S., Rong, L., Qi, C., Sun, C. and Wu, X. (2026) 'Distributed thermal storage for mitigating heat supply-demand imbalance in district heating systems: A thermohydraulic analysis', *Energy*, 348, 140479.

Yao, L., Wang, Z., He, N., Chen, Q., Hu, G., Sa, Q. and Nie, B. (2026) 'In-depth understanding synergistic characteristics of heat-fluid-mass transport in packed bed with large-size hierarchically porous heat storage module: in-situ experiments and numerical simulations', *Energy*, 343, 139781.

Zhou, W. (2025) Research on thermal characteristics and optimization of a high-temperature phase change thermal storage device. Master's thesis. Guizhou University.

COMSOL. (n.d.) *Packed bed latent heat storage*. Available at:
<https://cn.comsol.com/model/packed-bed-latent-heat-storage-76181>